

## AVHRR ARCHIVE AND PROCESSING FACILITY AT THE UNIVERSITY OF BERN: A COMPREHENSIVE 1-KM SATELLITE DATA SET FOR CLIMATE CHANGE STUDIES

*Fabia Hüsler<sup>1</sup>, Fabio Fontana<sup>2</sup>, Christoph Neuhaus<sup>1</sup>, Michael Riffler<sup>1</sup>,  
Jan Musial<sup>1</sup>, and Stefan Wunderle<sup>1</sup>*

1. University of Bern, Department of Geography, Bern, Switzerland;  
[fabia.huesler\(at\)giub.unibe.ch](mailto:fabia.huesler(at)giub.unibe.ch)
2. University of British Columbia, IRSS: Integrated Remote Sensing Studio,  
Department of Forest Resource Management, Vancouver, Canada

### ABSTRACT

Over the last few years an increasing need for full resolution, multi-temporal AVHRR data for climate studies has been identified. To serve the purpose of climate change monitoring, certain requirements in terms of data consistency and continuity specified by GCOS need to be met. The University of Bern has received and archived daily full resolution AVHRR data over Europe for the period 1984 to date and aims at the establishment of a high-quality fundamental climate data record in accordance with these requirements. In this paper, details on the data availability and processing system are given. A selected application on snow cover retrieval from historical AVHRR data shows encouraging results regarding the generation of long-term climatologies from different essential climate variables. It is concluded that the archive presented and the existing pre-processing hold a great potential for becoming a valuable tool for the analysis of environmental changes in the European Alps and adjacent regions.

### INTRODUCTION

#### Scientific context

The use of historical satellite data has become an attractive option to study changes in climate since they provide access to spatially and temporally comprehensive information on the entire earth surface. To ensure that high-quality data records necessary to address climate-related issues are defined, obtained and made available to all potential users, the Global Climate Observing System (GCOS) was founded by the World Meteorological Organization (WMO) in 1992. Within the framework of this project, satellite data were identified as a key component of global climate monitoring by reason of their essential contribution to determining atmospheric, oceanic and terrestrial climate variables (1). In contrast to other sources of information, remote sensing provides the unique opportunity to monitor various components of the Earth's system on a global scale with high temporal resolution. In this context, the global long-term data record of the National Oceanic and Atmospheric Administration (NOAA) and the European meteorological operational satellite system (MetOp) Advanced Very High Resolution Radiometer (AVHRR) is of particular interest.

Although products from newer generation sensors, e.g., from the Moderate Resolution Imaging Spectroradiometer (MODIS) sensor, have become available, AVHRR uniquely provides daily global coverage of the past 25 years, which makes it especially suitable for use in climate studies. Launched in 1978, the mission has been planned to be operational at least until 2020, based on NOAA Polar Orbiting Environmental Satellites (POES) as well as on MetOp satellites in cooperation with the European Organisation for the Exploitation of Meteorological Satellites (Eumetsat). Even though the payload of MetOp is rather different from the NOAA satellites, the mounted AVHRR/3 instrument is identical.

Despite the great potential of satellite observations, the use of AVHRR data in long-term studies has encountered serious challenges. Retrieved information must be used with caution in clima-

tological studies since non-target signal variability can introduce artificial trends into retrieved parameters. To serve the purpose of climate change monitoring, requirements concerning data continuity and consistency between different missions and instruments were established by GCOS (2). Many efforts have been undertaken to correct effects which are known to reduce the quality of the AVHRR data set, see e.g. (3,4,5,6,7), with the aim to achieve the AVHRR processing performance in accordance with the GCOS accuracy requirements.

### The AVHRR sensor and the data records

The AVHRR sensor is an imaging radiometer originally designed for meteorological and oceanic purposes. The instrument's nominal orbit altitude is approximately 833 km above the Earth's surface with a spatial resolution of 1.1 km at nadir and a swath width of 2700 km. Table 1 summarises the spectral characteristics of the AVHRR channels. Depending on the type of instrument, the sensor measures the reflected and emitted radiation in four (AVHRR/1), five (AVHRR/2), or six (AVHRR/3) spectral channels. While channels 1 and 2 are sensitive to reflected solar radiation, channels 4 and 5 are designed to measure the emitted terrestrial longwave radiation. Channel 3 of AVHRR/1-2, centred at 3.7  $\mu\text{m}$ , measures both reflected solar and emitted terrestrial radiation. On the latest instrument version, AVHRR/3 channel 3 is able to alternate between 1.6  $\mu\text{m}$  (3A) during daylight hours and 3.7  $\mu\text{m}$  (3B) during night. Further details on the AVHRR sensor design and engineering specifications are given in Cracknell (8), Kidwell et al. (9), Goodrum et al. (10), and Robel et al. (11).

*Table 1: Spectral characteristics of the different AVHRR sensors. All values are approximations and might vary from satellite to satellite.*

|         | NOAA-6,-8,-10             | NOAA-7,-9,-11,-12,-14     | NOAA-15,-16,-17,-18,-19, Metop-A |
|---------|---------------------------|---------------------------|----------------------------------|
| Channel | AVHRR/1 ( $\mu\text{m}$ ) | AVHRR/2 ( $\mu\text{m}$ ) | AVHRR/3 ( $\mu\text{m}$ )        |
| 1       | 0.58-0.68                 | 0.58-0.68                 | 0.58-0.68                        |
| 2       | 0.73-1.10                 | 0.73-1.10                 | 0.73-1.0                         |
| 3A      | -                         | -                         | 1.59-1.63                        |
| 3B      | 3.55-3.93                 | 3.55-3.93                 | 3.55-3.93                        |
| 4       | 10.50-11.50               | 10.30-11.30               | 10.30-11.30                      |
| 5       | Ch4 repeated              | 11.50-12.50               | 11.50-12.50                      |

Besides accomplishing the original design of the mission, the sensor has successfully been used to retrieve various other geophysical parameters such as vegetation indices (12), snow cover distribution (13), solar radiation budget (14), land and sea surface temperature (15,16), fire detection (17) and atmospheric applications including aerosol content (18,19) or cloud parameters (20).

Many satellite products with global coverage are available from AVHRR. Mostly, these data sets are based on the AVHRR Global Area Coverage (GAC) Level 1B data at a reduced spatial resolution, which is obtained through an onboard averaging scheme. This spatial sampling results in one pixel being representative for an area of the size of 3 km by 5 km at the sub-satellite point. Within the AVHRR Pathfinder programme, jointly administrated by NOAA and National Aeronautics and Space Administration (NASA), various products for land (21), atmospheric (22) and oceanic (23) applications were generated up to the hemispheric scale through the reprocessing of AVHRR GAC data collected since 1981. These records uniquely provide 25-year global satellite data and have been used in various climate studies, e.g., (24,25).

In addition to the GAC-based data sets and to take advantage of the full resolution of AVHRR, a project to generate a global 1-km data set was initiated in 1994 (26,27). The raw data was provided by several national and regional reception facilities. This remarkable international effort finally resulted in the production of a global 1-km data set compiled for the period 1992 to 1996 by the US Geological Survey (USGS) EROS Data Center. Although only the period 1992 to 1996 was processed, this project bears a great potential, and reprocessing and continuation is strongly recommended (28).

Apart from the global data sets, several 1-km AVHRR records for the use in climate change studies were generated at a smaller scale. For example, a comprehensive historical 1-km AVHRR baseline data record over Canada for the period 1981 to 2004 was produced at the Canada Center of Remote Sensing (CCRS; (6)). Another 1-km historical AVHRR data set was compiled for Southern Africa between 1985 and 1998 to extend a SPOT-VEGETATION derived Normalised Difference Vegetation Index (*NDVI*) time series back in time (29). In Europe, the full resolution AVHRR long-term terrestrial Mediterranean Extended Daily One Km AVHRR Data Set (MEDOKADS) is available for the use in land surface parameter studies (30). It covers the European continent for the period 1989 to approx. 2003. Concerning the atmospheric domain, the German Aerospace Center generated a 14-year cloud climatology from AVHRR data for the period 1990-2003 (31).

In addition to the data sets mentioned, a 25-year AVHRR data record for the use in climate research, at the full spatial resolution, has been processed by the Remote Sensing Research Group (RSGB) at the University of Bern, Switzerland. Due to the geographic location of Bern (46.93°N, 7.41°E), the research focus of RSGB has traditionally been on the European Alps. The complex topography of the region results in pronounced altitudinal gradients, which leads to highly variable climatic zones on short horizontal and vertical distances. Since Alpine ecosystems are very sensitive to climate change (32), they are considered to be particularly suitable for studies of a variety of phenomena on relatively small spatial scales. To complement ground station measurements, satellite observations provide a valuable tool to access comprehensive information in mountainous regions (33). This additional information is of particular interest for climate research in the Alpine Region where rapid environmental changes caused by shifts in temperature and precipitation patterns have been observed over the recent decades (34). Furthermore, the usefulness of AVHRR data over the Alpine Region is reported from investigations using coarse resolution GAC data, if adequate correction is applied (35). However, a more detailed data set without inducing the known limitations in the GAC resampling scheme (36) is assumed to deliver more accurate results in mountainous regions. Given the importance of mountain regions for climate change assessment combined with the strong need for full resolution AVHRR data sets for the use in climate research in general (37,38) a 1-km AVHRR data record over this region bears a high potential of providing valuable new information.

Hence, this paper presents and discusses the AVHRR data archive at the University of Bern in terms of data availability and processing. A selected application example derived from the data set is presented and remaining challenges with respect to long-term climatology compilation are outlined.

The paper is organised as follows: In section *Data* the data reception facility is described and the data availability is discussed. Section *Methods* outlines the data processing in detail and addresses remaining challenges concerning the generation of a long-term AVHRR data record. Section *Application Example* gives a short overview on an application of this data set. The last section concludes the paper with a summary and an outlook on future plans including processing, applications and data acquisition.

## DATA

### Data reception

The RSGB receives and archives NOAA and MetOp AVHRR data at the local receiving station in Bern, Switzerland (46.93°N, 7.41°E). Full resolution AVHRR data is read out daily from each operational platform in High Resolution Picture Transmission (HRPT) format. Depending on the satellite's status (<http://www.oso.noaa.gov/poesstatus/>), data from NOAA -12, -15, -17 (morning platforms) and -14, -16, -18, -19 (afternoon platforms) have been almost completely recorded over the last several years and the local reception is planned to continue until the expected end of the mission in 2020.

The reception frequency varies depending on the satellites in orbit and in 2004 reached up to 12 data sets within 24 hours when the number of functional NOAA platforms in orbit was at a maximum. Depending on the orbit, the maximum area recorded in each overpass ranges approximately from the Barents Sea (75°N) to the Libyan Desert (25°N) in the north-south direction and from the Canary Islands (15°W) to the Black Sea (40°E) in the east-west direction.

The raw data is received at 10 bit radiometric resolution and first converted to NOAA AVHRR Level 1B format. The data unpacking routine then extracts the raw digital counts, the calibration coefficients for the visible and the thermal channels for each image row as well as a grid file containing information on sun and sensor geometry and geographic tie points. This is the input to the data pre-processing system including radiometric correction, geometric rectification and cloud masking, specified in section *Methods*.

**Data archive**

The full archive is assembled from several different data sources. The major contribution of archived data originates from our own data set recorded since 1981. Due to limited storage capacity, only a subset covering the Alpine Region was archived until 1996. To provide full coverage prior to 1996, additional data have been acquired from the Freie Universität Berlin from 1989-2007 as well as from the Comprehensive Large Array data Stewardship System ([www.class.ncdc.noaa.gov](http://www.class.ncdc.noaa.gov)), formerly known as Satellite Active Archive, for the period 1989-2000 and particular missing scenes in other years. The period between 1984 and 1989 as well as remaining data gaps have been completed with morning passes obtained from the German Aerospace Center. Thanks to all these supplementary contributions the archive has successfully been extended back to 1984.

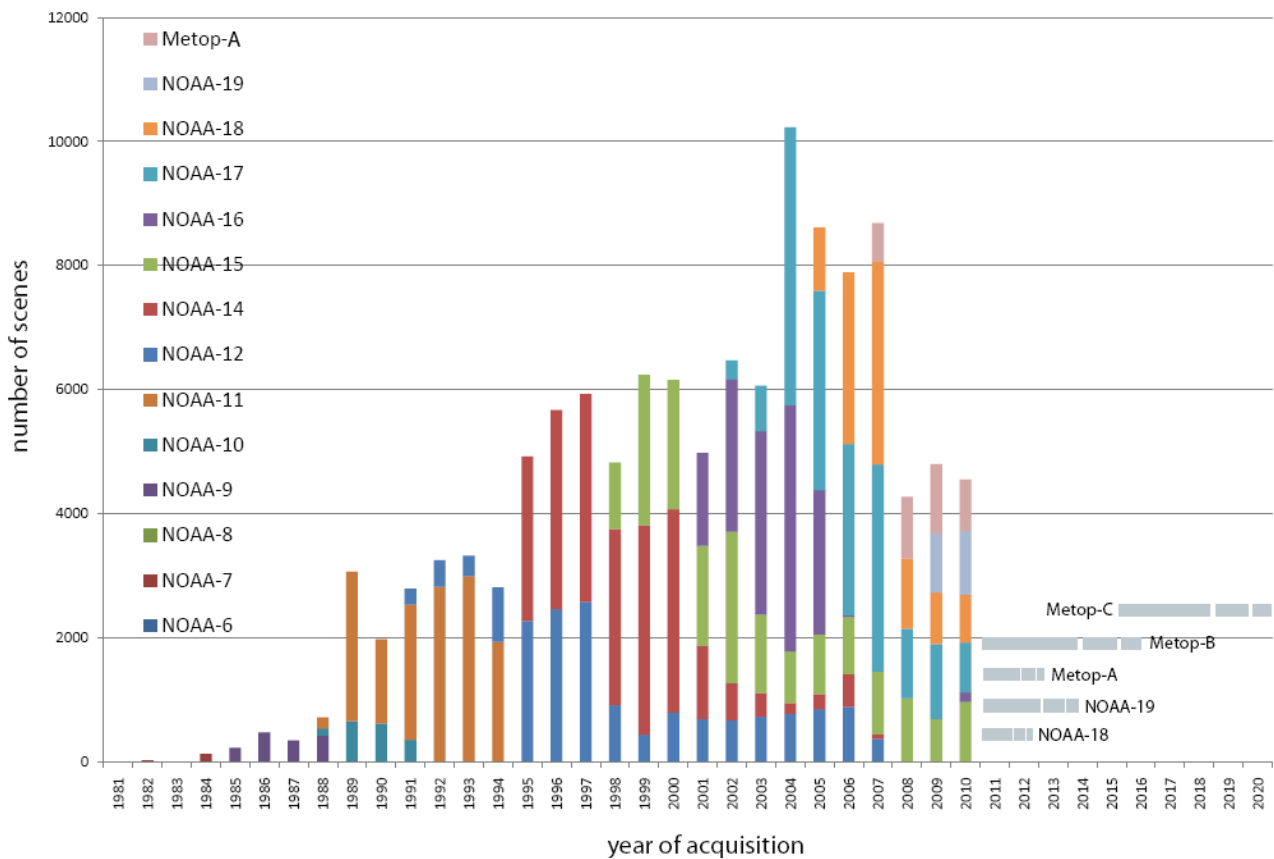


*Figure 1: The AVHRR data volume collected at the University of Bern illustrated by satellite mission and acquisition year. Grey bars indicate planned missions carrying a 'heritage' AVHRR/3 instrument onboard. A large number of orbit segments are available from 2002 onwards when contributions from different sources overlap.*

Figure 1 gives an overview of the archive components and planned missions by satellite platform and year of acquisition. The total number of 120,000 files corresponds to approximately 11 Terabytes of raw data. An irregular distribution over such an extended time frame is inevitable, for example, due to the maintenance of the receiving station or the reduced number of platforms in operation. It has been concluded that the amount of data available before 1984 is insufficient for use in long-term applications. While the number of files in 1984 and 1985 is of limited use, the record provides a spatially and temporally complete coverage after 1985. After 1995, the average number

of files per year has amounted to 6800. A peak of data availability was reached between 2004 and 2007 when up to six AVHRR platforms were simultaneously in orbit and archive contributions from different sources overlapped. As indicated in Figure 1, new satellites have already been launched and reached operational status (MetOp-A and NOAA-19) while others are planned (MetOp-B, MetOp-C) within the framework of the Initial Joint Polar-Orbiting Operational Satellite System (IJPS) that comprises a cooperation between NOAA and Eumetsat. These missions are intended to provide, foster and improve climate change monitoring by carrying 'heritage' instruments such as AVHRR/3 onboard to continue long-term environmental observations.

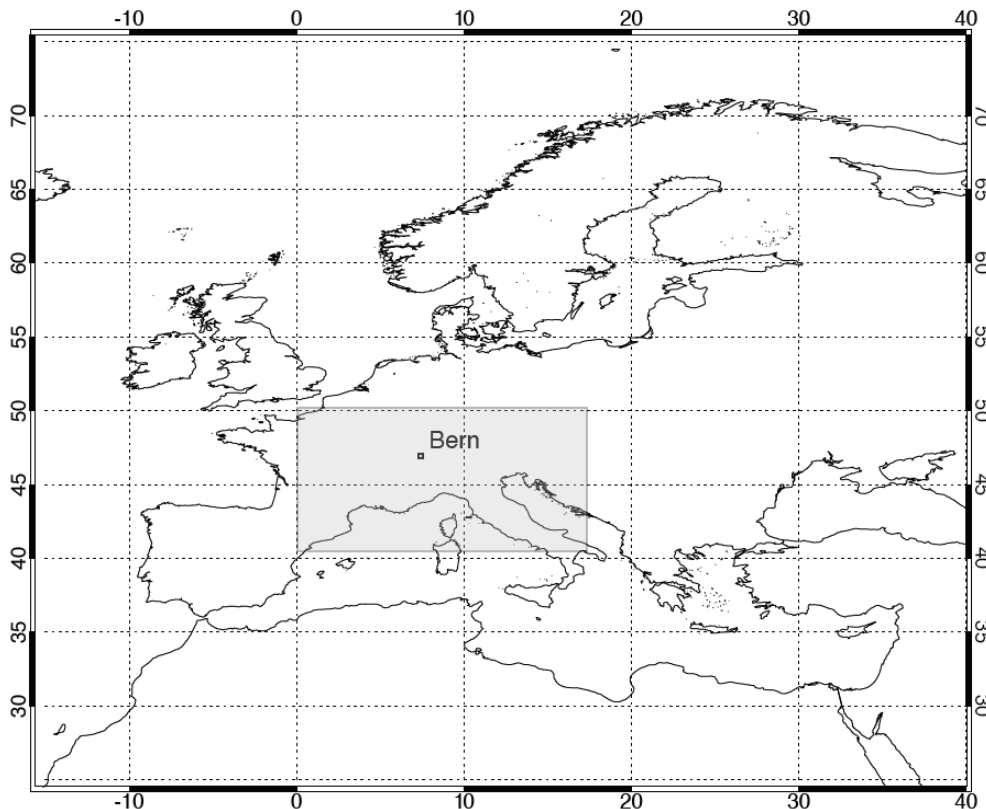


Figure 2: The geographic extent of the archived data set. The smaller frame indicates the Alpine Region subset on which the majority of the RSGB applications are based.

The full spatial coverage of the data set includes the geographic extent as illustrated in Figure 2. Within the shown boundary coordinates of  $-15^{\circ}\text{E}/75^{\circ}\text{N}$  (upper left corner) and  $40^{\circ}\text{E}/25^{\circ}\text{N}$  (lower right corner) both the full extent or a limited region of interest can optionally be defined for processing. The smaller frame in Figure 2 indicates the geographic extent of the greater European Alpine Region subset used for most applications at RSGB. All available scenes have been reprojected into geographic projection using the WGS84 spheroid, i.e. latitude - longitude information at a resolution of  $0.01^{\circ} \times 0.007^{\circ}$  is provided.

As required by GCOS, the data set provides suitable periods of overlaps for consecutive AVHRR sensors from NOAA-9 onwards. This offers the opportunity for intersatellite comparison in terms of calibration (see Figure 4) and viewing geometry with regard to a homogeneous long-term climate data record. Furthermore, repeated daily measurements from multiple sensors are provided to assess changes in the diurnal cycle of surface and atmospheric properties.

## METHODS

### Radiometric Calibration

Consistent and accurate calibration is essential to create a homogeneous satellite climate data record since physical quantities derived from different sensors need to be comparable. The AVHRR calibration process of the shortwave and thermal channels varies with respect to the avail-

ability of adequate calibration information. For the thermal channels, an onboard calibration information based on a view of stable blackbody and deep-space reference is provided, which is utilised to convert raw counts to a meaningful physical quantity: the brightness temperature. The infrared channels of the AVHRR/3 instrument are calibrated according to the KLM User's Guide (10) including the correction for detector nonlinearities. For AVHRR/2, a slightly modified method than the one suggested by Kidwell et al. (9) was applied. Namely, the nonlinear response of the channels 3B, 4 and 5 is corrected according to the method suggested by Walton et al. (39). This modification provides increased radiometric consistency by applying the same correction to all platforms. Figure 4c displays a time series of monthly mean brightness temperatures from AVHRR channel 4 from different platforms revealing no trend as well as a very high radiometric sensor-to-sensor consistency suggesting its suitability for climate change studies.

In contrast to the thermal channels, the visible and near-infrared channels are only calibrated pre-launch, which complicates the calibration procedure as their signal was observed to decrease over time (8). This problem was addressed soon after the beginning of the mission and, therefore, the degradation of the AVHRR sensitivity after launch has been widely discussed, e.g., (40,41,42). To account for this fact, time-dependent correction using updated calibration coefficients is required. Several sets of post-launch calibration coefficients derived from vicarious and inter-satellite calibration for different AVHRR sensors have been suggested in the literature (6,9,11,43,44,45,46,47,48,49) and joint projects to achieve comparability of physical measurements from different satellites were set up (38).

Here, we currently use the updated coefficients suggested by Heidinger et al.(49). Based on these updated coefficients, channels 1, 2 and 3A are calibrated to top-of-atmosphere (TOA) reflectance as described in the NOAA User's Guides (9,10,11). Within the Quality Assurance Framework of Earth Observation (<http://qa4eo.org>) a Catalogue of Worldwide Test Sites for Sensor Characterization was set up to assure calibration accuracy and enhance sensor intercomparability. To analyse the radiometric consistency of our data we used the La Crau test site (50), which is considered to be the radiometrically most stable target in Europe (Figure 3).

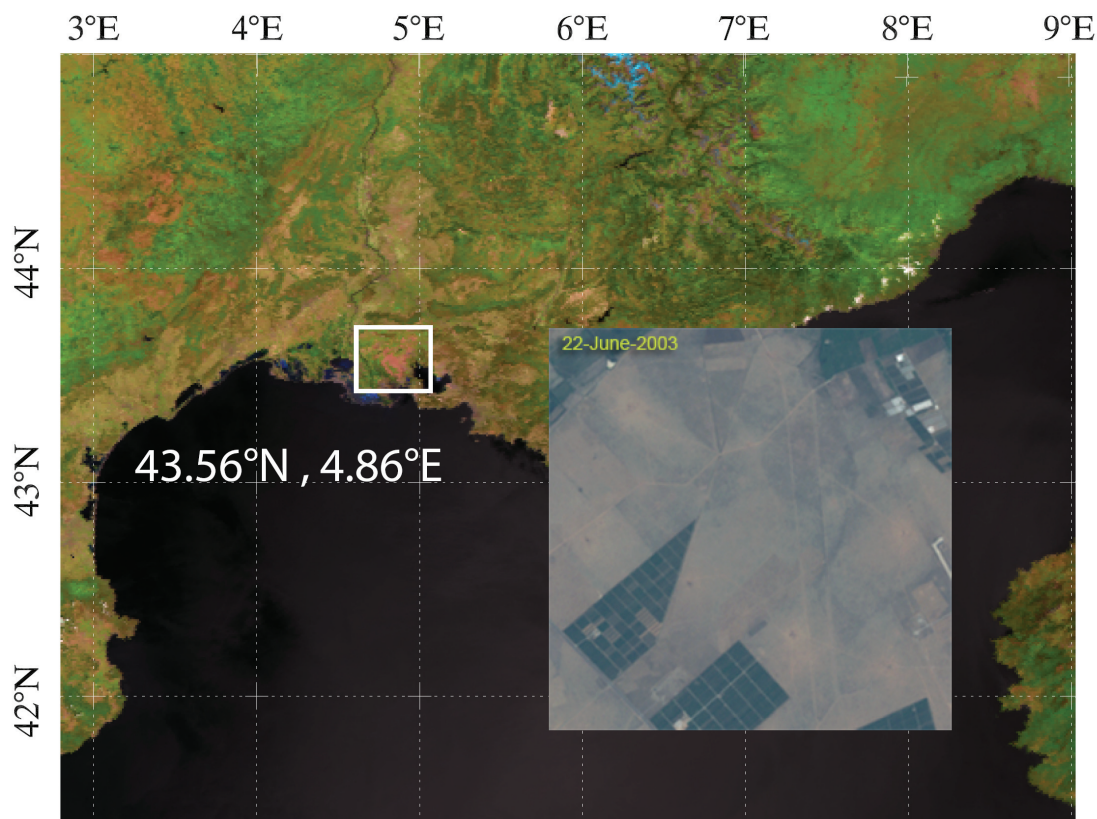


Figure 3: This subset shows the geographic location of the CEOS test site La Crau Sanddunes, France.

Figure 4 shows the TOA VIS (a) and NIR (b) monthly mean reflectance time series for the period 1989 – 2010 over the test site in Southern France. No systematic trend was found for the time series analysed. The variability is marginally higher for AVHRR Channel 2 reflectances and the standard deviations, even though showing a variation of up to  $\pm 0.02 \mu\text{m}$ , are mainly caused by a slight seasonal component and hence remain relatively constant over all platforms (Table 2). The variation is assumed to partly originate in variable acquisition and illumination geometry, remaining cloud and haze contamination, changing soil moisture conditions over the test site or even spurious contributions from a nearby vegetation cover indicating the target might not be completely temporally invariant (50). Nonetheless, the results shown in Figure 4a and b and Table 2 indicate a reasonable radiometric stability of the used post-launch calibration coefficients. A comparison to the coefficients suggested by the National Environmental Satellite, Data, and Information Service (NESDIS; <http://www.osdpd.noaa.gov/ml/ppp/notices.html>) calibrated time series revealed a slightly better performance of the PATMOS calibration. Especially NOAA-14 was found to have a systematic higher reflectance in both investigated channels (1 and 2) when calibrated with NESDIS coefficients.

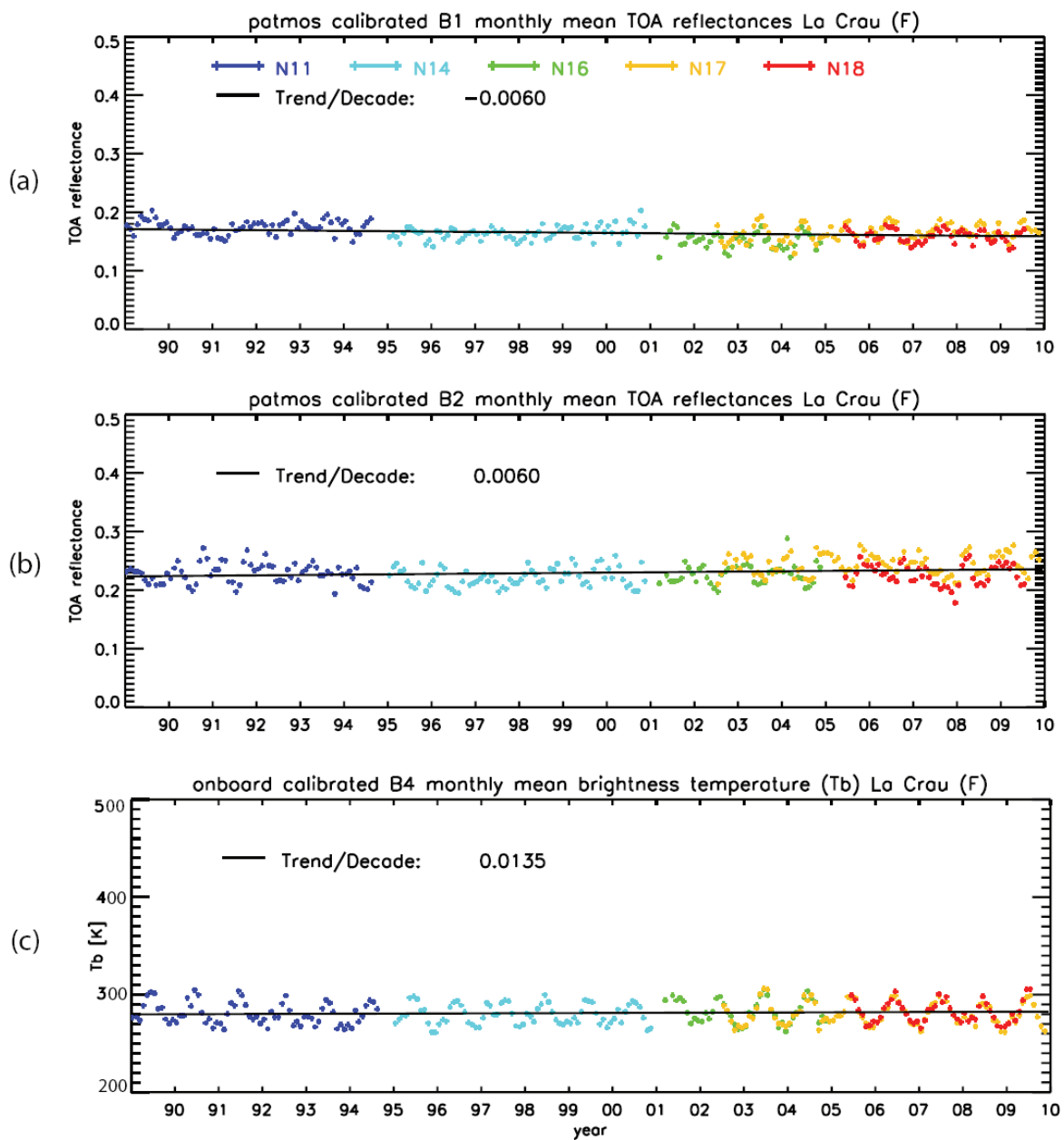


Figure 4: The time series of mean monthly TOA reflectance (and brightness temperature, respectively) derived from the AVHRR instrument measured over the radiometrically stable surface located in La Crau, France. AVHRR band 1 (a) band 2 (b) and band 4 (c).

*Table 2: Mean and standard deviations of TOA reflectance (Band 1 and 2) and for selected AVHRR sensors over La Crau (France).*

|         | Band 1 |       | Band 2 |       |
|---------|--------|-------|--------|-------|
|         | mean   | SD    | mean   | SD    |
| NOAA-11 | 0.174  | 0.012 | 0.230  | 0.017 |
| NOAA-14 | 0.164  | 0.011 | 0.222  | 0.016 |
| NOAA-16 | 0.152  | 0.014 | 0.227  | 0.016 |
| NOAA-17 | 0.164  | 0.014 | 0.244  | 0.017 |
| NOAA-18 | 0.159  | 0.011 | 0.225  | 0.018 |

As an independent step, Trishchenko et al. (5,51) recommended accounting for differing Spectral Response Functions (SRF) among various AVHRRs in long-term applications. This correction is done by the use of the suggested parameters of a quadratic best fit function referenced to NOAA-9 for channels 1 and 2 of each platform.

### **Geolocation**

Accurate geolocation remains critical for generating long-term data records for climate studies of land surface and atmospheric parameters, as has been emphasised in many previous studies, e.g., (6,52). Inaccurate co-registration of consecutive images may lead to biases in time series analyses since every single scene contributes to the final product (53).

Geolocation schemes for AVHRR solely based on orbital models lead to a geolocation accuracy of 1-4 km at the sub-satellite point. Known errors in image navigation based on orbit parameters result from inaccuracies in orbital models, satellite clock timing errors and deviations in satellite attitude angles (52). Better geolocation precision for AVHRR can only be achieved by a combination of ephemeris data with chip refining.

In the automated image navigation scheme outlined here, a first geometric approximation is carried out based on ephemeris data obtained from the Two-Line Elements/Simplified General Perturbations (TLE/SGP) model from the North American Aerospace Defence (NORAD). Since the accuracy is strongly influenced by the time shift between effective overflight time and orbit model parameters (6,54), the orbital model parameters closest to the acquisition time are taken to predict the exact position and velocity of the spacecraft. To avoid errors caused by the unprecise satellite clock, three different time servers are used for a precise external time signal. Based on this information and assuming the satellite attitude angles to be zero, the geographic location viewed by the sensor can be determined within a few kilometers. Figure 5a exemplarily illustrates the geolocation accuracy of a NOAA-17 scene achieved by orbit model image navigation. Compared to the expected reference coastlines and lakeshores (ENVI Version 4.3, ITT Industries, Inc.), a shift of a few kilometres along the orbital track is observed. This accuracy is not sufficient for climate data records and additional georeferencing steps are required.

To account for deviations of the spacecraft attitude angles, which were assumed to be zero in the first step, a land feature based correction of image navigation parameters (roll, pitch, yaw and time) is included (55). Due to this attitude correction, a geolocation accuracy close to one pixel is obtained.

For the following feature matching procedure a predefined Ground Control Points (GCPs) library is implemented. Additional GCPs are defined based on a random search process, if the number of GCPs accepted from the library does not exceed a predefined threshold. The GCPs on the reference image are defined as locations with the highest spatial variability estimated by the variance of the reflectance. Consequently, the position of a GCP is determined at the image location where the correlation between a rectified reference image map and an image sub-window (currently set at 21 x 21 pixels) is highest. Considering the found GCP's (a minimum of 50 points is required for the image to be processed) the image grid is then adjusted using the best fitting second order polynomial coefficients. Finally, the original AVHRR scene is rectified according to the corrected grid by nearest neighbour resampling.

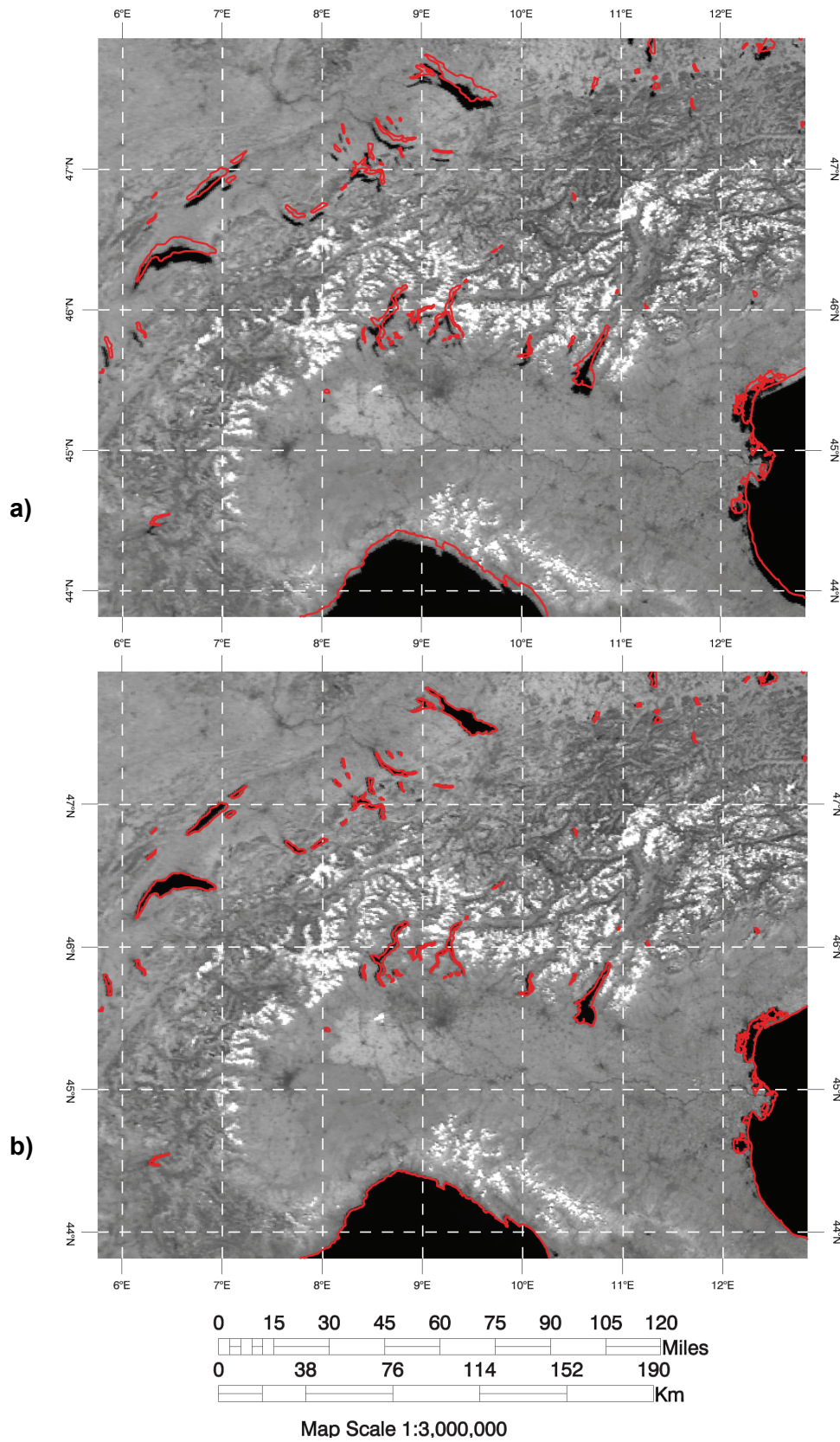


Figure 5: Georeferencing accuracy of the NOAA-17 AVHRR scene from 26 July 2007 at 09:54 UTC over the European Alps by means of orbit model navigation (a) achieving a geolocation precision of a few kilometres and feature matching procedure to accomplish subpixel agreement (b) between land-water boundaries and the reference coastlines (red colour). The map scale is 1:3'000'000.

As mentioned previously, the European Alps have traditionally been in the focus of research at RSGB. Due to the influence of elevated topography on the geometric accuracy of AVHRR data, an additional processing step is required. Depending on terrain elevation and viewing geometry, pixels may be displaced by up to a few kilometres. Neglecting this displacement may lead to important biases in AVHRR data over mountainous terrain (36). Therefore, an automated orthorectification procedure using a 1-km spatial resolution Digital Elevation Model (DEM) corrects for these displacement errors. For each pixel, this orthoshift is calculated based on its surface elevation divided by the tangent of the satellite elevation angle (56) and corrected accordingly. This process finally results in the imagery that provides both the image-based information of the original scene and the accurate geodetic map coordinates.

The overall georeferencing accuracy is shown in Figure 5b. The shift as seen in Figure 5a is corrected by the additional referencing steps (GCP refinement and orthorectification) resulting in a subpixel precision. The land-water boundaries are in much better agreement with the reference coastlines. The overall geolocation accuracy of this data set was further confirmed by the ability to determine lake water surface temperature of small Alpine lakes (57).

### Cloud Masking

An adequate cloud mask is a prerequisite for satellite applications because accurate retrieval of surface parameters greatly depends on an accurate cloud/no cloud discrimination. The cloud masking procedure has been crucial since the earliest retrievals of this kind of datasets and thus an extensive set of methodologies for derivation of cloud masks have been proposed. The SPARC (Separation of Pixels Using Aggregated Rating over Canada) algorithm capitalises on findings of many previous studies (58). It was tailored to work with the data acquired by any generation of the AVHRR sensor mounted onboard of the NOAA satellites starting from the NOAA-6 to the latest NOAA-19. Its design allows working all year round, day and night over the temperate and polar regions. It utilises all five spectral channels of the AVHRR instrument, as well as surface skin temperature maps and a land/water mask. The special feature of the SPARC algorithm is related to computation of an aggregated rating, which accumulates the results of several tests. Furthermore, this score may be converted to the specific mask under user-dependent constraints. Apart from the cloud mask this algorithm also produces additional layers, discriminating snow/ice and cloud shadow areas. All characteristics mentioned above make the SPARC algorithm the most robust and flexible in comparison to other existing schemes for derivation of the cloud cover from AVHRR data.

The SPARC cloud masking algorithm is based on three types of tests: the brightness temperature test in channel 4, which produces the T score; the reflectance brightness test in channel 1 (VIS), which produces the B score; and the reflectance test in channel 3 (A or B), which produces the R score. In the first one the brightness temperature B4 is compared with a dynamical threshold derived from the surface skin temperature data provided by the European Centre for Medium-Range Weather Forecasts (ECMWF) as well as by MeteoSwiss (COSMO model). The second test is a surface brightness analysis in channel 1 (VIS) over land and in channel 2 (NIR) over water. The third test is more complex, because it is based on channels 3A/3B, which are used interchangeably and therefore two independent approaches are required here. In case of channel 3B, which includes both thermal and solar flux components, the reflectance is calculated from the radiance. For channel 3A a specific function was designed, which relates the 3A reflectance to the reflectance in the first channel. The singular scores from corresponding tests adjusted by an offset term are then constructed in a way that negative values are assigned to cloud-free pixels whereas positive refer to overcast ones. The scaling factor applied to each test modifies its significance in the overall score. If the rating value is close to zero then additional tests are performed in order to classify a pixel with an increased level of confidence. Those additional tests include: simple ratio test in the first two channels, texture and thermal uniformity examination and thin cirrus test based on a difference in brightness temperatures between the channel 4 and the channel 5. For a more detailed description of the scores and their computation we refer to Khlopnev and Trishchenko (58). The last set of correction factors is applied to the final rating in order to enhance the classification results. They account for:

1. snow condition: when the distinction between snow and clouds in the first two channels of the AVHRR sensor is difficult. This correction factor is based on the comparison between skin surface temperature and the freezing point temperature, which is defined as a sine function oscillating between a maximum of 2°C in the spring season and a minimum of -2°C in the fall. The more negative the difference is ( $T_{surf} - T_{freeze}$ ) the higher the probability that the area is covered by snow, thus the scale factor is penalised with low value.
2. sun glint effect over water, which affects the reflectance tests: This correction factor is derived from the angular relationship between satellite angle, relative azimuth and minimises the overall contribution of B, R and N scores.
3. day-night transition zone: because of the high sun zenith angle the reflectance in the first three channels may be overestimated due to the properties of the surface bidirectional reflectance distribution function.

The shadow detection scheme that has been merged with the SPARC algorithm was proposed by Simpson et al. (59). It utilises spectral properties of cloud shadows as well as some geometrical assumption based on the solar zenith, viewing zenith and the relative azimuth angles. Additionally, the shadow length was corrected by an estimation of the cloud top height, which is performed by analysing the temperature differences between the surface brightness in channel 4 and the ground data.

Figure 6 depicts an application example of two cloud masking algorithms: SPARC and CASPR (Cloud and Surface Parameter Retrieval; (60)), applied to AVHRR winter scene acquired by NOAA-16 on 4th of January 2004. It could be seen that both algorithms work well, however, SPARC does not introduce misclassified pixels over the snow in the Alpine region as well as at the image top.

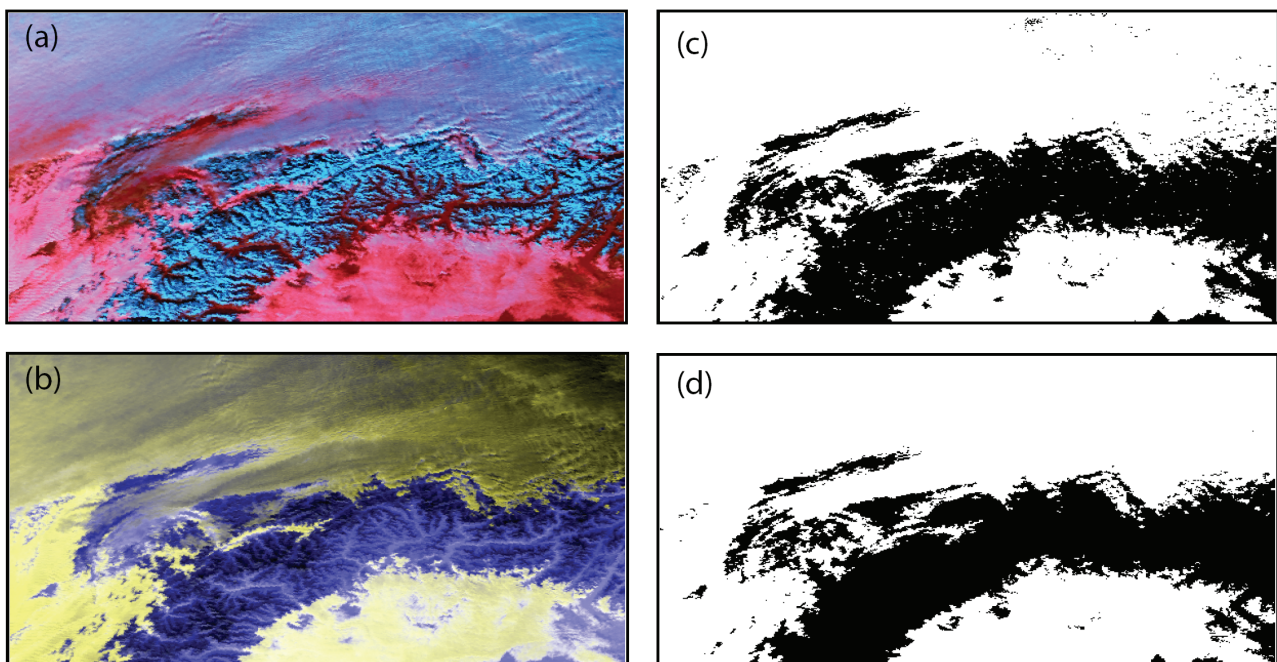


*Figure 6: The accuracy of the implemented cloud masking algorithms. The AVHRR scene presented was acquired by NOAA-16 on 4 January 2004. Panel a) presents the false colour composite generated from reflectance in channel 3B (red), channel 2 (green), channel 1 (blue). Clouds are depicted in colours ranging from pink to light blue depending on droplet size. Intensive blue colour corresponds to snow cover. Panel b) presents the false colour composite generated from brightness temperature in channel 3B (red), channel 3B (green), channel 4 (blue). Areas depicted in blue colours represent a cloud-free terrain. Panel c) presents the previously used CASPR cloud mask with some obviously misclassified pixels within the Central Alps and the northern border of the image while panel d) presents SPARC cloud mask with a more accurate pixel discrimination.*

## Post-processing

After the data is processed as outlined, the output product consists of radiometrically and geometrically corrected channel information: TOA reflectance for channels 1, 2 and 3A (AVHRR/3) and brightness temperature for channel 3 (AVHRR/2), 3B (AVHRR/3), 4 and 5. Additional information on viewing geometry and cloud contamination is provided for each pixel.

Certain analyses of geophysical parameters such as snow and ice cover or some limited vegetation dynamic applications can be carried out with the pre-processed data set. For most applications, however, further processing of the data is required. For example, the atmospheric impact especially on products derived from the shortwave AVHRR channels (e.g. *NDVI*) can be significant (61,62). An accurate correction for this effect must be implemented in the data processing to convert calibrated TOA reflectances to surface reflectance values. The atmospheric correction applied here is based on the Simplified Method for Atmospheric Correction (SMAC; (63)) radiative transfer code updated to 6S (64). The requested input parameters are the angular information on viewing and sun geometry, obtained from the data itself, as well as atmospheric parameters like ozone, sea level pressure and water vapour. These are taken from the reanalysis data provided by ECMWF. Furthermore, the Aerosol Optical Depth (*AOD*) is needed for the correction. Since comprehensive ground-based *AOD* information for the full period is not yet available, the *AOD* is successfully retrieved from the archive itself (19).

Another aspect that needs to be addressed is the varying illumination and viewing geometry for anisotropic surfaces, characterised by the Bidirectional Reflectance Distribution Function (*BRDF*) (65,66). Even though several standardisation methods have been suggested (e.g. (67)), such correction can be difficult to achieve reliably over longer time periods and across large areas (68). As for various applications, the suggested compositing scheme including only the forward or backward scattering hemisphere, respectively, is used to address this problem (69). Furthermore, we are currently implementing, adapting and validating the AMBRALS (the Algorithm for Modeling [MODIS] Bidirectional Reflectance Anisotropies of the Land Surface; (70)) code, which includes several kernel-driven semi-empirical *BRDF* models (71). Among these kernels the Ross-Thick-Li-Sparse (*RTLS*) can be specified and used for AVHRR and MODIS processing taking into account the volumetric, geometric and isotropic scattering. The application of these models require a good sampling of illumination and viewing angles in zenith and azimuth, respectively. The directional sampling of surface reflectances from AVHRR can only be obtained by the accumulation of sequential observations over a specified time period. These angles are covered by our multi-day clear sky composites. The defined *BRDF*-shapes are then selected based on landcover type. Depending on cloud coverage over the region a backup algorithm will be used to avoid jeopardising the approach with insufficient samplings. But an advantage of the selected *BRDF* models is the high accuracy with sparse directional samplings (72). Likewise, this correction also removes, to a large degree, the impact of orbital drift, discussed in detail in Gutman (73), which also introduces variable imaging geometries and therefore needs careful consideration in long-term AVHRR data analyses.

## APPLICATION EXAMPLE

The main intention of this paper is to focus on the documentation of the available data and the pre-processing methods. First studies (namely snow and aerosol time series) are ongoing and will be subject to upcoming publications. Nevertheless, in order to present the potential of the data archive acquired by the University of Bern, we exemplarily present a preliminary time series of the snow cover area percentage over Switzerland for the period 1986-2010.

Snowcover applications based on AVHRR data have a long tradition at RSGB since vast parts of Switzerland are directly affected by snow cover related processes such as water management, ecosystem dynamics, hydropower generation, tourism and natural hazards. Furthermore, snow cover also plays a vital role in climate studies in mountainous regions since it strongly affects the radiation budget and surface heat transfer. One parameter, which is of great interest, is the spatial snow cover extent and its variability over the last decades. Historical data collected from the

AVHRR sensor can provide the longest comprehensive record of the spatial snow cover extent at a detailed resolution of 1 km.

Snow detection is carried out simultaneously to the cloud masking procedure described in detail in section *Cloud Masking*. As outlined, the SPARC algorithm includes a snow detection part, which is basically performed using the T, B and R score. Several threshold tests are used to ensure that a pixel is sufficiently bright (B score), the discrimination between snow and clouds is carried out by limiting the R score to small values and the T score is employed to ensure that the brightness temperature at 10.8  $\mu\text{m}$  is close to the predicted surface skin temperature. If a pixel passes all threshold tests it is classified as potentially snow covered and cloudfree. To enhance the results in the complex terrain of the Alpine Region some refinements, namely threshold adaptations based on landcover and a topographic shadow modelling, were additionally implemented. A more detailed description of the algorithm and an extensive validation of the snow product can be found in Hüsler et al. (74). To diminish the problem of frequent cloud cover over the region, a 10-day compositing procedure using the last cloud-free observation within the time interval was applied for further analyses.

Figure 7 depicts a preliminary time series of the snow area percentage in Switzerland as derived from the presented archive. Despite some small data gaps, that were filled applying a spatio-temporal filling algorithm suggested by Kondrashov und Ghil (75), the time series can provide a complete overview on the spatial variations of the snow cover extent over the last 25 years.

No trend analyses or climatological interpretations have been conducted yet since an extensive validation study including a sensor-to-sensor consistency assessment is carried out and will be subject to an upcoming publication (74). Based on this, a clear indication of potential uncertainties can be provided with the final time series of different snow related parameters.

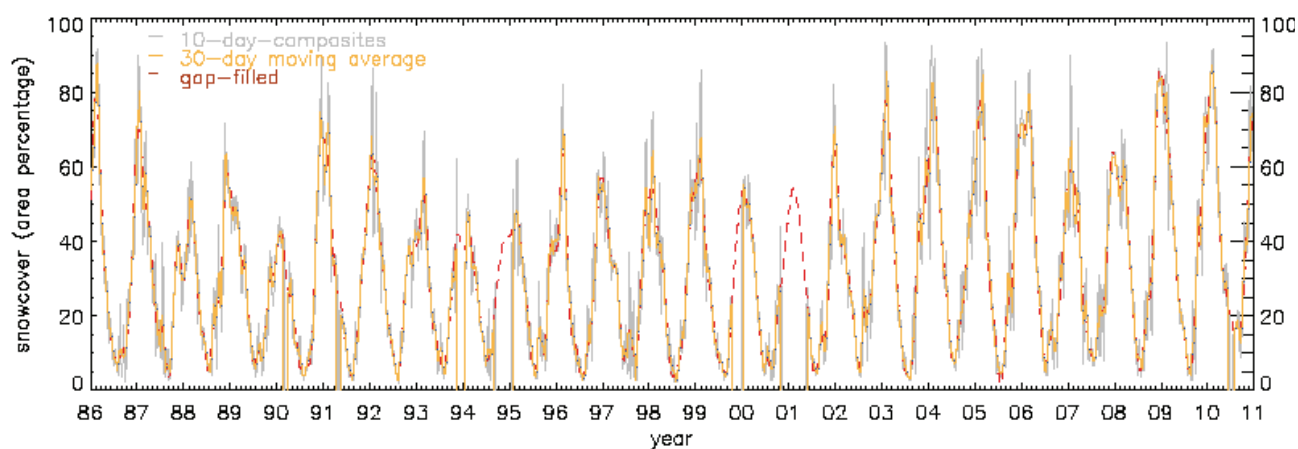


Figure 7: Preliminary time series of AVHRR data employed to derive the snow cover area percentage in Switzerland for the period 1986-2010 based on 10-day image composites (grey line). The orange solid line represents the 30-day running mean. Gaps were filled applying a spatio-temporal filling algorithm (75) illustrated with the red dashed line.

## CONCLUDING REMARKS

Long-term continuous satellite data sets are of great importance for climate research, which is why the AVHRR data record hosted at the RSGB was presented in terms of data availability and state of data processing. The data set is calibrated using up-to-date information on post-launch calibration indicating reasonable radiometric consistency in the visible as well as in the thermal channels. The automated geolocation procedure relying on ephemeris data navigation combined with a chip matching achieves subpixel accuracy. Cloud masking is carried out using a robust and stable algorithm, applicable to all historical and current platforms, rendering an aggregated probability rating of cloud contamination rather than a yes/no decision. A specific application example showing the snow cover area percentage in Switzerland over the archived time period (1986-2010) illustrates the potential of the data set and the existing algorithms. At the time of writing, this archive repre-

sents the only known automatically navigated, orthorectified and full resolution AVHRR data record over Europe covering more than 20 years.

Given the importance of mountainous regions for climate change studies, this archive bears the potential of becoming an important tool for the analysis of environmental changes in the Alpine Region and entire Europe. Based on the presented expertise concerning mountain remote sensing, future applications can not only be expanded to other mountain ranges (e.g. Pyrenees, Scandinavia) within the archived subset but algorithms can be applied to similar AVHRR data sets in other regions of the world (e.g. Tibet).

The accuracy of the retrieved parameters, especially from older sensors, will continue to be assessed and derived products will be carefully validated with data sets of well-known quality and an adequate measurement period. Especially over Switzerland, the high quality ground-based observations offer a great opportunity for extensive validation in cooperation with the Federal Office of Meteorology and Climatology MeteoSwiss (for albedo and phenology), the Swiss Federal Institute for Forest, Snow and Landscape Research (WSL; for snow cover), and AERONET (for AOD). Moreover, also complementary space/air-borne information such as MODIS or Landsat data not restricted to Switzerland as well as aerial imagery (provided by Federal Office of Topography swisstopo) will be used.

In the near future, we aim at presenting a consistent and systematically validated 25-year time series compiled from the RSGB 1-km AVHRR data set covering great parts of Europe including quality flags and uncertainty estimates for all derived parameters. The data processing is currently further extended to provide a record that serves as a fundamental climate data record in complete accordance with the GCOS accuracy requirements. The final objective is to provide a high-quality data set for reliably studying different aspects of surface and atmosphere as well as for serving for climate model calibration. Furthermore, data assimilation and blended products combining data derived from different sensors and homogenising them is very desirable. This can help to assess many new information by benefiting from the advantages of AVHRR as well as from the new technologies of the newer high-quality sensors (29,76).

Concerning the time span of the record, it is planned to access additional data to extend the archive back in time (1981-1988) by acquiring data from other European research agencies such as Dundee Satellite System, UK or the Earth Observation Center of DLR, Germany. This, however, involves considerable financial resources. For future AVHRR data acquisition, new satellites have already been launched and have reached operational status (MetOp-A and NOAA-19) while others (MetOp-B and MetOp-C) are foreseen within the framework of the Initial Joint Polar-Orbiting Operational Satellite System (IJPS) that comprises a cooperation between NOAA and Eumetsat. These missions are intended to provide, foster and improve climate change monitoring by carrying 'heritage' instruments such as AVHRR/3 to continue long-term environmental observations. The RSGB reception of AVHRR data will be continued until the end of the mission. By then, the archive will consist of a 35-year satellite data record.

In conclusion, the unique value of AVHRR satellite information from the continuously growing data record at the RSGB will contribute to significantly enhance the understanding of past, present and future changes in climate variables not only for the European Alps, but, in the near future, also for the entire area of Europe.

## **ACKNOWLEDGEMENTS**

The authors would like to thank Dr. Dirk Koslowsky from the Freie Universität Berlin for the generous NOAA AVHRR data supply. The provision of data from NOAA Comprehensive Large Array-data Stewardship System and the German Aerospace Center is gratefully acknowledged. The authors also would like to thank Dr. Andrew K. Heidinger for the latest Patmos-X calibration coefficients and MeteoSwiss for the COSMO data supply. We also would like to thank the three anonymous reviewers for their valuable comments on the manuscript. The publication was supported by the Foundation Marchese Francesco Medici del Vascello.

**REFERENCES**

- 1 World Meteorological Organization, 2004. [Implementation Plan for the Global Observing System for Climate in Support of the UNFCCC](#), 29 pp. (last date accessed: 24 Aug 2011)
- 2 Global Climate Observing System, 2008. Systematic observation requirements for satellite-based products for climate. [Supplemental details to the satellite-based component of the Implementation Plan for the Global Observing System for Climate in Support of the UNFCCC](#). 103 pp. (last date accessed: 24 Aug 2011)
- 3 James M E & S N V Kalluri, 1994. The Pathfinder AVHRR Land Data Set - An Improved Coarse Resolution Data Set For Terrestrial Monitoring. [International Journal of Remote Sensing](#), 15(17): 3347-3363
- 4 Vermote E, N EL Saleous, Y J Kaufman & E Dutton, 1997. Data pre-processing: Stratospheric aerosol perturbing effect on the remote sensing of vegetation: Correction method for the composite NDVI after the Pinatubo Eruption. [Remote Sensing Reviews](#), 15: 7-21
- 5 Trishchenko A P, J Cihlar, & Z Li, 2002. Effects of spectral response function on surface reflectance and NDVI measured with moderate resolution satellite sensors. [Remote Sensing of Environment](#), 81(1): 1-18
- 6 Latifovic R, A Trishchenko, J Chen, W Park, K Khlopenkov, R Fernandes, D Pouliot, Cn Ungureanu, Y Luo, S Wang, A Davidson & J Cihlar, 2005. Generating Historical AVHRR 1 km Baseline Satellite Data Records over Canada Suitable for Climate Change Studies. [Canadian Journal of Remote Sensing](#), 31(5): 324-346
- 7 Pedelty J, S Devadiga, E Masuoka, M Brown, J Pinzon, C Tucker C, D Roy, Ju Junchang, E Vermote, S Prince, J Nagol, C Justice, C Schaaf, Liu Jicheng, J Privette & A Pinheiro, 2007. Generating a Long-term Land Data Record from the AVHRR and MODIS Instruments. [IGARSS: 2007 IEEE International Geoscience and Remote Sensing Symposium](#), 1-12; 1021-1024
- 8 Cracknell A P, 1997. *The Advanced Very High Resolution Radiometer* (Taylor & Francis) 534 pp.
- 9 Kidwell K B, 1998. [NOAA Polar Orbiter Data \(POD\) User's Guide](#) (TIROS-N, NOAA-6, -7, -8, -9, -10, -11, -12, -13 and -14). (last date accessed: 24 Aug 2011)
- 10 Goodrum G, K B Kidwell & W Winston, 2000. [NOAA KLM User's Guide](#). (last date accessed: 1 Sept 3011)
- 11 Robel J, 2009. [NOAA KLM User's Guide with NOAA-N,-P Supplement](#) (last date accessed: 24 Aug 2011)
- 12 Myneni R B, C D Keeling, C J Tucker, G Asrar & R R Nemani, 1997. Increased plant growth in the northern high latitudes from 1981 to 1991. [Nature](#), 386: 698-702
- 13 Romanov P, G Gutman & I Csiszar, 2000. Automated monitoring of snow cover over North America with multispectral satellite data. [Journal of Applied Meteorology](#), 39(11): 1866-1880
- 14 Hucek R & H Jacobowitz, 1995. Impact of scene dependence on AVHRR albedo models. [Journal of Atmospheric and Oceanic Technology](#), 12(4): 697-711
- 15 McClain E P, W G Pichel & C C Walton, 1985. Comparative performance of AVHRR-based multichannel sea surface temperatures. [Journal of Geophysical Research](#), 90: 11587-11601
- 16 Becker F & Z L Li, 1990. Towards a local split window method over land surfaces. [International Journal of Remote Sensing](#), 11(3): 369-393
- 17 Lasaponara R, V Cuomo, M F Macchiato & T Simoniello, 2003. A self-adaptive algorithm based on AVHRR multitemporal data analysis for small active fire detection. [International Journal of Remote Sensing](#), 24(8): 1723-1749

- 18 Ignatov A & L Stowe, 2002. Aerosol retrievals from individual AVHRR channels. Part II: Quality Control, Probability Distribution Functions, Information Content, and Consistency Checks of Retrievals. Journal of the Atmospheric Sciences, 59(3): 335-362
- 19 Riffler M, C Popp, A Hauser, F Fontana & S Wunderle, 2010. Validation of a modified AVHRR aerosol optical depth retrieval algorithm over Central Europe. Atmospheric Measurement Techniques, 3(5): 1255-1270
- 20 Rossow W B & R A Schiffer, 1990. Advances in understanding clouds from ISCCP. Bulletin of the American Meteorological Society, 80(11): 2261-2287
- 21 Zhao H & R Fernandes, 2009. Daily snow cover estimation from Advanced Very High Resolution Radiometer Polar Pathfinder data over Northern Hemisphere land surfaces during 1982-2004. Journal of Geophysical Research, 114(D5): D05113
- 22 Stowe L L, H Jacobowitz, G Ohring, K R Knapp & N R Nalli, 2002. The Advanced Very High Resolution Radiometer (AVHRR) Pathfinder Atmosphere (PATMOS) climate dataset: Initial analyses and evaluations. Journal of Climate, 15(11): 1243-1260
- 23 Reynolds R W, N A Rayner, T M Smith, D C Stokes & W Q Wang, 2002. An improved in situ and satellite SST analysis for climate. Journal of Climate, 15(13): 1609-1625
- 24 Gutman G, 1994. Global data on land surface parameters from NOAA AVHRR for use in numerical climate models. Journal of Climate, 7: 669-680
- 25 Tucker C J, J E Pinzon, M E Brown, D A Slayback, E W Pak, R Mahoney, E F vermonte & N El Saleous, 2005. An extended AVHRR 8-km NDVI dataset compatible with MODIS and SPOT vegetation NDVI data. International Journal of Remote Sensing, 26(20): 4485-4498
- 26 Eidenshink J C & J L Faundeen, 1994. The 1 km AVHRR global land data set: first stages in implementation. International Journal of Remote Sensing, 15(17): 3443-3462
- 27 Townshend J R G, C O Justice, D Skole, J P Malingreau, J Cihlar, P Teillet, F Sadowski & S Ruttenberg, 1994. The 1 km resolution global data set: needs of the International Geosphere Biosphere Programme. International Journal of Remote Sensing, 15(17): 3417-3441
- 28 Teillet PM, N El Saleous, M C Hansen, J C Eidenshink, C O Justice & J R G Townshend, 2000. An evaluation of the global 1-km AVHRR land dataset. International Journal Of Remote Sensing, 21(10): 1987-2021
- 29 Swinnen E & F Veroustraete, 2008. Extending the SPOT-VEGETATION NDVI time series (1998-2006) back in time with NOAA-AVHRR data (1985-1998) for South Africa. IEEE Transactions on Geoscience and Remote Sensing, 46: 558-572
- 30 Koslowsky D, 2003. The MEDOKADS data set as a substantial part of a remote sensing data network for a Mediterranean research and application network. In: Bolle H-J, editor. Mediterranean Climate: Variability and Trends (Berlin: Springer Verlag) p.165-177
- 31 Meerkötter R, C König, P Bissolli, G Gesell & H Mannstein, 2004. A 14-year European Cloud Climatology from NOAA/AVHRR data in comparison to surface observations. Geophysical Research Letters, 31(15): 4pp.
- 32 Beniston M, 2003. Climatic change in mountain regions: A review of possible impacts, Climatic Change, 59: 5-31
- 33 Bugmann H, A B Gurung, F Ewert, W Haeberli, A Guisan, D Fagre, A Kääh, and GLO-CHAMORE participants, 2007. Modeling the biophysical impacts of global change in mountain biosphere reserves. Mountain Research and Development, 27(1): 66-77
- 34 Organe consultatif sur les changement climatiques, 2002. Das Klima ändert - auch in der Schweiz. Die wichtigsten Ergebnisse des dritten Wissensstandberichts des IPCC aus der Sicht der Schweiz (last date accessed: 24 Aug 2011)

- 35 Stöckli R & P L Vidale, 2004. European plant phenology and climate as seen in a 20 year AVHRR land-surface parameter dataset. International Journal of Remote Sensing, 25: 3303-3330
- 36 Fontana F, A P Trishchenko, K V Khlopenkov, Y Luo & S Wunderle, 2009. Impact of orthorectification and spatial sampling on maximum NDVI composite data in mountain regions. Remote Sensing of Environment, 113(12): 2701-2712
- 37 Cihlar J, J Chen, Z Li, R Latifovic, G Fedosejev, M Adair, W Park, R Fraser, A Trishchenko, B Guindon, D Stanley & D Morse, 2002. GeoComp-n, an advanced system for the processing of coarse and medium resolution satellite data. Part 2: Biophysical products for Northern ecosystems. Canadian Journal of Remote Sensing, 28(1): 21-44
- 38 CEOS, 2006. [Satellite Observations of the Climate System: The Committee on Earth Observation Satellites \(CEOS\) response to the Global Climate Observing System \(GCOS\) Implementation Plan \(IP\)](#). 54 pp. (last date accessed: 29 Aug 2011)
- 39 Walton C C, J T Sullivan, C R N Rao & M P Weinreb, 1998. Corrections for detector nonlinearities and calibration inconsistencies of the infrared channels of the Advanced Very High Resolution Radiometer. Journal of Geophysical Research, 103(C2): 3323-3337
- 40 Rao N, 1987. Pre-Launch Calibration of Channels 1 and 2 of Advanced Very High Resolution Radiometer. NOAA Technical Report NESDIS, 36, 62 pp.
- 41 Price J C, 1988. An update on visible and near infrared calibration of satellite instruments. Remote Sensing of Environment, 21: 24419-422
- 42 Holben B N, Y J Kaufman & J D Kendall, 1990. NOAA-11 AVHRR visible and near-IR inflight calibration. International Journal of Remote Sensing, 11(8): 1511-1519
- 43 Kaufman Y J & B N Holben, 1993. Calibration of the AVHRR visible and near-IR bands by atmospheric scattering, ocean glint and desert reflection. International Journal of Remote Sensing, 14(1): 21-52
- 44 Teillet P M & B N Holben, 1994. Towards operational radiometric calibration of NOAA AVHRR imagery in the visible and near-Infrared channels. Canadian Journal of Remote Sensing, 20(1): 1-10
- 45 Rao C R N, 1995. Inter-satellite calibration linkages for the visible and near-infrared channels of the Advanced High Resolution Radiometer on the NOAA-7, -9 and -11 spacecraft. International Journal of Remote Sensing, 16(11): 1931-1942
- 46 Vermote E & Y J Kaufman, 1995. Absolute Calibration of AVHRR Visible And Near-Infrared Channels Using Ocean And Cloud Views. International Journal of Remote Sensing, 16(13): 2317-2340
- 47 Mitchell R M, D M O'Brien & B W Forgan, 1996. Calibration of the AVHRR shortwave channels: II Application to NOAA 11 during early 1991. Remote Sensing of Environment, 55(2): 139-152
- 48 Rao C R N & J Chen, 1999. Revised post-launch calibration of the visible and near-infrared channels of the Advanced Very High Resolution Radiometer (AVHRR) on the NOAA-14 spacecraft. International Journal of Remote Sensing, 20(18): 3485-3491
- 49 Heidinger A K, W C Straka, C C Molling, J T Sullivan & X Q Wu, 2010. Deriving an inter-sensor consistent calibration for the AVHRR solar reflectance data record. International Journal of Remote Sensing, 31(24): 6493-6517
- 50 Rondeaux G, M D Steven, J A Clark & G Mackay, 1998. La Crau: A European test site for remote sensing validation. International Journal of Remote Sensing, 19(14): 2775-2788

- 51 Trishchenko A P, 2009. Effects of spectral response function on surface reflectance and NDVI measured with moderate resolution satellite sensors: Extension to AVHRR NOAA-17, 18 and METOP-A. Remote Sensing of Environment, 113, 335-341
- 52 Rosborough G W, D G Baldwin & W J Emery, 1994. Precise AVHRR image navigation. IEEE Transactions on Geoscience and Remote Sensing 32(3): 644-657
- 53 Townshend J R G, C O Justice, C Gurney & J McManus, 1992. The impact of misregistration on change detection. IEEE Transactions on Geoscience and Remote Sensing, 30(5): 1054-1060
- 54 Vallado D A, P Crawford, R Hujsak & T Kelso, 2006. [Revisiting spacetrack report No.3: Revision 1](#), 92 pp. (last date accessed: 29 Aug 2011)
- 55 Crawford P, 2005. Software Manual Landmark Navigation Correction (Crawford Space Communications Ltd.) 25 pp.
- 56 Voigt S, 2000. Advanced methods for operational mapping of Alpine snow cover using medium resolution optical satellite data. Dissertation, University of Bern, 91 pp.
- 57 Oesch D C, J M Jaquet, A Hauser & S Wunderle, 2005. Lake surface water temperature retrieval using Advanced Very High Resolution Radiometer and Moderate Resolution Imaging Spectroradiometer data: Validation and feasibility study. Journal of Geophysical Research, 110C12014
- 58 Khlopenkov K V & A P Trishchenko, 2007. SPARC: New cloud, snow, and cloud shadow detection scheme for historical 1-km AVHRR data over Canada. Journal of Atmospheric and Oceanic Technology, 24(3): 322-343
- 59 Simpson J J, T McIntire, J Zhonghai & J R Stitt, 2000. Improved cloud top height retrieval under arbitrary viewing and illumination conditions using AVHRR data. Remote Sensing of Environment, 72(1): 95-110
- 60 Key J R, 2002. [The Cloud and Surface Parameter Retrieval \(CASPR\) System for Polar AVHRR - User's Guide](#), 36 pp. (last date accessed: 1 Sept 2011)
- 61 Holben B N, 1986. Characteristics of maximum-value composite images from temporal AVHRR data. International Journal of Remote Sensing, 7(11): 1417-1434
- 62 Cihlar J, D Manak & M D'Iorio M, 1994. Evaluation of compositing algorithms for AVHRR data over land. IEEE Transactions on Geoscience and Remote Sensing, 32(2): 427-437
- 63 Rahman H & G Dedieu, 1994. SMAC: A simplified method for the atmospheric correction of satellite measurements in the solar spectrum. International Journal of Remote Sensing, 15(1): 123-143
- 64 Vermote E F, D Tanré & J J Morcrette, 1997. Second Simulation of the Satellite Signal in the Solar Spectrum, 6S: An Overview. IEEE Transactions on Geoscience and Remote Sensing, 35(3): 675-686
- 65 Nicodemus E F, 1970. Reflectance nomenclature and directional reflectance and emissivity. Applied Optics, 9(6): 1474-1475
- 66 Cihlar J, R Latifovic, J Chen, A P Trishchenko, Y Duc, G Fedosejevs & B Guindon, 2004. Systematic corrections of AVHRR image composites for temporal studies. Remote Sensing of Environment, 89(2): 217-233
- 67 Los S O, P R J North, W M F Grey & M J Barnsley, 2005. A method to convert AVHRR Normalized Difference Vegetation Index time series to a standard viewing and illumination geometry. Remote Sensing of Environment, 99(4): 400-411
- 68 Donohue R J, M L Roderick & T R McVicar, 2008. Deriving consistent long-term vegetation information from AVHRR reflectance data using a cover-triangle-based framework. Remote Sensing of Environment, 112(6): 2938-2949

- 69 Luo Y, A P Trishchenko & K V Khlopenkov, 2008. Developing clear-sky, cloud and cloud shadow mask for producing clear-sky composites at 250-meter spatial resolution for the seven MODIS land bands over Canada and North America. Remote Sensing of Environment, 112(12): 4167-4185
- 70 Wanner W, X Li & A H Strahler, 1995. On derivation of kernel-driven models of bidirectional reflectance. Journal of Geophysical Research, 10(D10): 21077-21089
- 71 Roujean J L, M Leroy & P Y Deschamps, 1992. A bidirectional reflectance model of the Earth's surface for the correction of remote sensing data. Journal of Geophysical Research, 97(18): 20455-20468
- 72 Jin Y F, C B Schaaf, F Gao, X W Li, A H Strahler, W Lucht & S L Liang, 2003. Consistency of MODIS surface bidirectional reflectance distribution function and albedo retrievals: 1. Algorithm performance. Journal of Geophysical Research - Atmosphere, 108(D5): 4158
- 73 Gutman G G, 1999. On the monitoring of land surface temperatures with the NOAA/AVHRR: removing the effect of satellite orbit drift. International Journal of Remote Sensing, 20(17): 3407-3413
- 74 Hüsler F, T Jonas, S Wunderle & S Albrecht, 2011. Validation of a modified snow cover retrieval from historical 1-km AVHRR data over the European Alps for climate research purposes. In preparation for Journal of Geophysical Research.
- 75 Kondrashov D & M Ghil, 2006. Spatio-temporal filling of missing points in geophysical data sets. Nonlinear Processes in Geophysics, 13, 151-159
- 76 Liang D, 2009. Issues in Bayesian Gaussian Markov Random Field Models with Application to Intersensor Calibration. Dissertation, University of Iowa, 198 pp.